GPS Solutions (2024) 28:119
https://doi.org/10.1007/s10291-024-01655-1

ORIGINAL ARTICLE

On the real-time tropospheric delay estimates using low-cost GNSS receivers and antennas

Luohong Li[1,2,3] · Hongxing Zhang[1] · Yunbin Yuan[1] · Matthias Aichinger-Rosenberger[3] · Benedikt Soja[3]

Received: 15 December 2023 / Accepted: 5 April 2024

Abstract

Dense Global Navigation Satellite System (GNSS) observations are beneficial for monitoring the small-scale troposphere turbulence in both spatiotemporal domains. Densification of current geodetic GNSS networks can be achieved by incorporating low-cost GNSS receivers and antennas, benefitting weather monitoring. This study aims to focus on real-time tropospheric delay estimation using real-time GNSS data streams collected by low-cost GNSS receivers and antennas. The results indicate that: (1) Low-cost GNSS devices can offer accuracies of 7.5 mm in winter and 10.8 mm in summer for real-time zenith tropospheric delay (ZTD) estimations; (2) By applying the phase center variation corrections for low-cost GNSS antennas, which are often ignored in previous studies on low-cost GNSS applications, can produce more reliable real-time ZTD estimations; (3) Low-cost GNSS devices can capture the ZTD fluctuations under heavy precipitation events in a real-time mode, showing a great potential as sensors to monitoring severe weather. These results underscore the viability of low-cost GNSS devices as cost-effective sensors that complement geodetic GNSS equipment in real-time troposphere monitoring and forecasting, especially at small scales. Their integration aids in the densification of existing monitoring networks, thereby bolstering GNSS meteorology applications.

Keywords Real-time · Low-cost GNSS receivers · Phase center variation · Zenith tropospheric delay · Severe rainfall

Introduction

The zenith tropospheric delay (ZTD) serves as a fundamental tropospheric parameter in Global Navigation Satellite System (GNSS) meteorology (Bevis et al. 1992). Advancing precise forecasts for severe weather requires high-resolution and (near) real-time updating observing systems (Guerova et al. 2016; Jones et al. 2020; Pottiaux 2009). Ground-based GNSS technology can provide accurate ZTD in real time with high spatiotemporal resolution for numerical weather prediction (NWP), thus playing a pivotal role in investigating meteorological processes (Dousa and Vaclavovic 2014; Du et al. 2023; Gendt et al. 2004; Li et al. 2015; Wang et al. 2022; Wilgan et al. 2023). However, the high cost and complex maintenance of geodetic GNSS receivers contradict the necessity for dense deployment in weather monitoring, potentially hindering the broader utilization of GNSS technology (Krietemeyer et al. 2020).

Fortunately, advancements in GNSS chipsets and algorithms designed to overcome hardware limitations have facilitated the widespread use of low-cost devices in atmospheric monitoring (Zangenehnejad and Gao 2021; Zhao et al. 2021). Low-cost receivers have shown great potential in sensing atmospheric parameters densely at a cheap price and can be considered a mature complement to geodetic receivers in traditional fields, such as troposphere and ionosphere modeling at a regional scale (Marut et al. 2022; Paziewski 2021; Wu et al. 2022). For example, space/ground-based dense sensor networks including low-cost GNSS devices can also contribute to the tropospheric tomography retrievals at global/local scale (Moeller 2022). Besides, they even show high potential for emerging

✉ Hongxing Zhang
caszhx@whigg.ac.cn

1 State Key Laboratory of Geodesy and Earth's Dynamics, Innovation Academy for Precision Measurement Science and Technology (APM), Chinese Academy of Sciences (CAS), Wuhan, People's Republic of China

2 College of Earth and Planetary Sciences, University of Chinese Academy of Sciences, Beijing, People's Republic of China

3 Institute of Geodesy and Photogrammetry, ETH Zurich, 8093 Zurich, Switzerland

Published online: 02 May 2024

applications, such as retrieving the soil moisture and vegetation optical depth using GNSS-Interferometric Reflectometry (GNSS-IR) (Humphrey and Frankenberg 2023; Karegar et al. 2022). Low-cost GNSS devices have a greater contribution to these applications in the future.

Many affords have been done in estimating ZTD using low-cost GNSS receivers (Barindelli et al. 2018; Bosser et al. 2022; Wu et al. 2022). Krietemeyer et al. (2018) retrieved ZTD from single-frequency GNSS receivers with a quality similar to that of geodetic receivers. Stępniak and Paziewski (2022) demonstrated the performance of tropospheric estimates using low-cost GNSS devices in postprocessing mode, where the differences between the low-cost and geodetic receivers that share a low-cost antenna are only 1.7–1.8 mm. Bosser et al. (2023) account for integrated water vapor (IWV) using a low-cost permanent GNSS network in France and the low-cost results are high correlations of the time series registered by nearby geodetic receivers. As for low-cost GNSS networks, Marut et al. (2022) established a very dense network in the city of Wroclaw, Poland, for retrieval of ZTD and IWV using 16 low-cost GNSS stations and validation results show satisfactory performance of the proposed low-cost setups, reaching smaller than 9 mm in standard deviation (STD) against troposphere final products from International GNSS Service (IGS). Aichinger-Rosenberger et al. (2023) also initiated a low-cost GNSS network in Switzerland, namely, MPG-NET, for monitoring environmental parameters such as water vapor and soil moisture. These networks provide opportunities and platforms for verifying the long-term performance of low-cost receivers and studying algorithms for troposphere data assimilation using mixed networks. The research on sensing of the troposphere using low-cost receivers would contribute to the deployment of low-cost receivers in monitoring networks and the performance of new combination networks.

However, most previous studies have been conducted in a postprocessing mode using geodetic networks, establishing a high-precision ZTD model for Precise Point Positioning (PPP) and used for water vapor monitoring (Huang et al. 2021; Lu et al. 2023, 2016). The investigation of real-time performance in estimating tropospheric parameters using low-cost receivers and antennas is lacking. The real-time performance is important for meteorological monitoring and short-term prediction. It has been taken account that the impact of low-cost GNSS antenna phase center variation corrections (PCVs) on the tropospheric estimates in Krietemeyer et al. (2018, 2020), showing the receiver can achieve high-quality ZTD estimations while the quality of the receiving antenna would limits the ZTD result. In addition, it is very common that low-cost antennas without known PCVs, such as u-blox ANN antenna, are equipped with low-cost receivers when deploying them into existing GNSS networks. The impact of PCVs of low-cost antenna should be accounted for and handled. Besides, the analysis of low-cost receivers in connection with severe weather events has also been less reported in previous works, especially in real-time mode. The literature also lacks a discussion of the conflict between rapid changes in the ZTD and the quality of estimated parameters in typical weather conditions. Rapid sensing of tropospheric changes, even under extreme weather conditions, is a major task for ground-based GNSS when low-cost devices can be potential devices to enhance the ground network. Thus, we aim to investigate the real-time performance of low-cost receivers in in severe weather events.

In this study, we seek to address the above problems and challenges concerning estimating tropospheric parameters using low-cost GNSS devices in real-time mode. First, the impact of low-cost antenna PCVs on ZTD estimations is also analyzed and discussed in postprocessing mode. Second, the ZTD results estimated using low-cost GNSS receivers and antennas in real-time mode are validated against final products and postprocessing results. Finally, the real-time response of low-cost GNSS devices in severe weather conditions is presented. In the following sections, we start by describing the datasets used in this study, continue with an introduction of the methodology and processing strategies, and conclude with the analysis of the ZTD results driven by low-cost receivers and their performances under rain event.

Data collection

In the experiment, static GNSS data were collected from a total of 7 stations. These stations comprised both low-cost receivers and neighboring geodetic receivers, each equipped with varying grades of antennas. The data collection spanned two weeks from June 19th to July 3rd, 2023 (170–184 in Day Of Year, DOY), representative of summer conditions. Additionally, another two-week period between October 27th and November 10th (DOY 300–314) was selected to represent winter conditions. The data collection sites encompassed the Jiufeng Mountains and the Donghu Campus of the Innovation Academy for Precision Measurement Science and Technology (APM) in Wuhan.

Table 1 provides comprehensive details regarding the receivers and antennas of seven GNSS stations. Notably, the distances between JFNG (IGS station, geodetic), JFTA (geodetic), and JFSP (low-cost) atop Jiufeng Mountain are all under 20 m, with small height difference between these stations, enabling direct comparison of ZTD values among them. As for Donghu Campus, stations APMB3S (geodetic), APMB3T (geodetic), and APMM (low-cost) are situated on the rooftop of Building No.3 (ten stories high), while UBUU (geodetic) resides atop a seven-story building. The

Table 1 Detailed information of receivers and antenna used

Name	Receivers	Antenna		Location
JFSP	Septentrio mosaic_X5 (low-cost)	CNTAT360 (low-cost)	None	Jiufeng mountain
JFTA	Trimble alloy (geodetic)	TRM159900.00 (geodetic)		
JFNG	Trimble alloy (geodetic)	TRM59800.00 None (geodetic)		
APMM	Septentrio mosaic_X5 (low-cost)	CNTAT360 (low-cost)	HXCS	Donghu campus
APMB3S	Septentrio POLARX5TR (geodetic)	HXCCGX601A (geodetic)		
APMB3T	Trimble alloy (geodetic)	UA35 (low-cost)		
UBUU	Trimble alloy (geodetic)	CHCC220GR CHCD (geodetic)		

winter campaign necessitated the removal of APMB3S and APMB3T due to setup change.

The Trimble Alloy and Septentrio POLARX5TR represent typical geodetic receivers, while the Septentrio mosaic-X5 is a cost-effective, robust multi-GNSS chip capable of tracking multiple frequencies and GNSS systems. While a standard geodetic setup (including receivers and antennas) surpasses $20,000, low-cost equipment account for less than five percent of this expense. The configuration utilized for low-cost monitoring stations costs approximately $700. Various grades of antennas are employed in low-cost applications. The AT360, a cost-effective antenna from COMNAV Company priced at $110, and the U35 is another low-cost antenna without PCVs. Details about the PCVs of AT360 are available on the Antenna Calibrations Website of NGS (https://www.ngs.noaa.gov/ANTCAL/#). The CHCA220GR, an alloy choke ring antenna with a dome, and other Trimble antennas represent typical geodetic

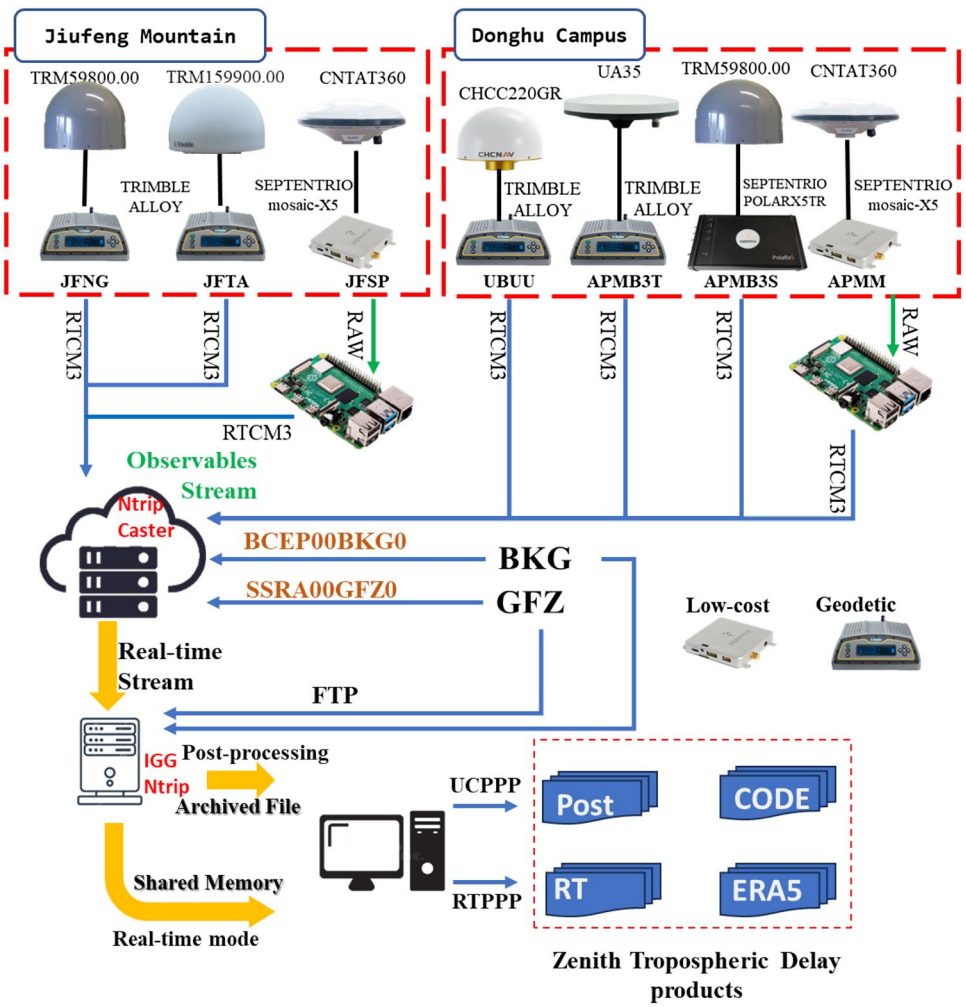

Fig. 1 Real-time and postprocessing flow chart of ZTD calculation using low-cost and geodetic GNSS receivers based on real-time stream. The real-time streams of GNSS observations are archived as RINEX files for postprocessing mode, while simultaneously being stored as shared memory for real-time PPP using IGG-NTRIP software

antennas used in the IGS network. Figure 1 illustrates the ZTD calculation flowchart with low-cost and geodetic GNSS devices in both real-time and postprocessing modes.

The low-cost receivers are connected to the microprocessor Raspberry Pie 4B and 4G router, which are used for remote controlling, monitoring, and transferring the GNSS raw data based on Radio Technical Commission for Maritime Services (RTCM) and the Networked Transport of RTCM via Internet Protocol (NTRIP). The geodetic receivers can broadcast their real-time stream (RTS) in RTCM format with built-in software when accessible to Internet. The real-time state-space representation (SSR) product of the GNSS orbit and clock, along with code biases, namely, SSRA00GFZ0, is generated and distributed by German Research Centre for Geosciences (GFZ). The NTRIP caster also is used to receive and distribute the RTS data. Real-time observation data, broadcast ephemeris and SSR corrections are received, decoded and archived as RINEX files by IGG-NTRIP, a well-developed software package for RTCM- and NTRIP-based real-time GNSS data streams processing at APM.

The final tropospheric ZTD products provided by the Center for Orbit Determination in Europe (CODE) are used as references to evaluate the performance of real-time ZTD. The CODE products are estimated by Bernese GNSS software 5.5 with an interval of 1 h for more than 300 globally distributed GNSS stations. The accuracy of the CODE final ZTD products is at a level of 4 mm, with respect to the tropospheric products generated by other measurement techniques such as VLBI, DORIS and radiosondes (Dach et al. 2009).

The fifth-generation reanalysis model (ERA5) is the latest climate reanalysis model from the European Centre for Medium-Range Weather Forecasts (ECMWF), replacing ERA-Interim. ERA5 takes both physical models and observations into account to describe the state of the atmosphere numerically (Hersbach et al. 2020). The ERA5 products with 37 pressure layers are utilized with a horizontal resolution of $0.25° \times 0.25°$ and a temporal resolution of 1 h (https://cds.climate.copernicus.eu), which can be accessible with a latency of 5 days. ZTD values are calculated from hourly ERA5 reanalysis fields using the station coordinate as input, which serve for comparison with the ZTD values from CODE final products and low-cost receivers in a rain severe weather event.

The precipitation data is provided by the Hubei Provincial Meteorological Bureau and collected hourly at the Wuhan national basic meteorological station (114.05 °E, 30.60 °N), which can collect and archive the basic meteorological elements to represent Wuhan City. It is also the nearest meteorological station to APM. Ground-based precipitation data is used to show the suitability of low-cost GNSS devices in monitoring fast-changing ZTDs under heavy precipitation.

The antenna PCVs information is vital for precisely estimating GNSS-based ZTD (Krietemeyer et al. 2020). The PCVs information of the geodetic GNSS antennas is available via the official antenna file released by IGS. However, the corresponding information on the low-cost antenna has received little attention and is possibly ignored in current studies on tropospheric delay estimating using low-cost GNSS devices.

Methodology

The GNSS data collected by low-cost and geodetic receivers are both processed using in-house parallel-running PPP software. The processing strategies used in the PPP software in both real-time and postprocessing modes are summarized in Table 2.

The performance of our PPP software for estimating GNSS-ZTDs in both postprocessing and real-time modes has been validated in previous studies in (Zhang et al. 2022) by comparing the numerical results with independent ZTD products from multiple-source techniques. The current updates and improvements mainly focus on real-time PPP algorithms and strategies, supporting GNSS data processing from geodetic receivers to low-cost receivers and antennas.

Results

In this section, we first illustrate the impacts of PCVs on ZTD estimations with low-cost GNSS devices. The accuracy and stability of the low-cost GNSS devices in estimating real-time ZTDs are assessed during a four-week period in a realistic real-time mode. Finally, the performance of low-cost GNSS receivers in estimating high-updating ZTDs in severe weather conditions is evaluated.

Impacts of low-cost antenna PCVs on GNSS-ZTD estimates

We selected the CODE final troposphere products as our reference to assess the accuracy of our postprocessing solutions and to evaluate the influence of antenna Phase Center Variations (PCVs). To ensure an accurate comparison, we extracted and compared data only from common epochs, eliminating the impact of interpolation on the evaluation results.

The receiver antenna significantly affects tropospheric estimates. The distinction between low-cost and geodetic scenarios primarily lies in the hardware of the receiver and antenna. Geodetic setups typically feature pre-calibrated

Table 2 Processing strategies used in PPP software

Items	Postprocessing mode	Strategies real-time mode
Observations	GPS/BDS-3 raw pseudorange and phase observables	
Frequency usage	L1/L2 for GPS and B1I/B3I for BDS-3	
orbit and clock	GFZ final products	SSRA00GFZ0
Sampling rate	30 s	1 s
Ambiguities	Float	
Estimator	Kalman filter (smooth)	Kalman filter (forwards)
	A priori precisions of 0.003 and 0.6 m for the phases and codes in the zenith direction	
Weighing strategy	$\sigma=\sigma_0\sqrt{1+4\cos^8 e}$(Hadas et al. 2020)	
Elevation cut-off angle	5°	
Phase center variation	igs14.atx	
Ionospheric delay	Estimated as white noise	
Station coordinates	Estimated as constant	
Zenith wet delay	Estimated as random-walk noise (10^{-8} m^2/s)	
	Estimated every 24 h	
Tropospheric gradients	$m_g(e) = \frac{1}{\sin(e)\tan(e)+C}$(Chen & Herring 1997)	
Mapping function	GMF	GMF

antenna PCVs, while low-cost antennas often lack this calibration information. Hence, it is crucial to consider the potential adverse effects of antenna PCVs on tropospheric estimates, especially in scenarios involving low-cost hardware. In cases where low-cost receivers are added to supplement existing GNSS networks, they often have low-cost receivers equipped with low-cost antennas that lack effective PCVs information. The difference of PCVs on low-cost and geodetic observables can cause inconsistency in the estimated tropospheric parameters.

For our analysis, we processed the postprocessing troposphere products of JFSP (low-cost) and JFTA (geodetic) stations, both with and without corrected antenna PCVs. We compared these results with the CODE final products near the JFNG station, effectively evaluating the impact of antenna PCVs on tropospheric estimates.

Figure 2 shows the cumulative distribution of ZTD differences of JFTA and JFSP against CODE, respectively. When PCVs are neglected, we found that an average bias of over 2 mm occurs in the ZTD from JFSP with the AT360 antenna, while average biases of over 4 mm occur at the JFTA station with the geodetic choke rings (TRM59800.00C) antenna. After applying the PCVs, the mean bias of ZTD differences is reduced by around 70% against the CODE final product, and low-cost estimates achieve a mean of 0.8 mm. The differences to CODE have been reduced. It is crucial that the antenna is correctly installed and oriented for PCVs, pointing north and placed horizontally. Flexibly obtaining and applying PCVs for a low-cost station would be a focus before deploying them with geodetic receivers in a monitoring network, potentially impacting ZTD consistency.

Simultaneously, incorporating knowledge of the PCVs of low-cost antennas or accounting for precise PCVs with a robot arm could be solutions for low-cost situations. We plan to conduct this experiment in the future. Nevertheless, integrating knowledge about PCVs of low-cost antennas is the preferred solution for achieving centimeter accuracy in sensing tropospheric parameters.

In Fig. 3, we present the four-week length time series of postprocessing ZTD estimates from JFSP (low-cost) and JFTA (geodetic), along with the ZTD time series of JFNG (geodetic) from CODE products in summer and winter campaign. It is evident that the postprocessing results show good agreement between our final ZTD and CODE products, regardless of whether it is geodetic receivers or low-cost receivers, as a small bias can be observed in mean of ZTD difference.

The mean difference in ZTD from JFTA (Trimble Alloy) is 2.6 mm, while the low-cost solutions (JFSP) have an average difference of 0.8 mm in summer. Conversely, the mean difference of ZTD is around 2 mm in winter. Both the RMS (Root Mean Square) and STD (Standard Deviation) values of our solutions compared to CODE are below 8 mm. These values are slightly reduced in winter, showing STD of around 5–6 mm in ZTD. ZTDs obtained from the two setups, specifically ALLOY + TRM59800.00C (JFTA) and Mosaic-X5 + AT360 (JFSP), exhibit high agreement. The results from JFSP (low-cost) are closer to the CODE final product than those of JFTA (geodetic), possibly due to multipath affecting the geodetic receiver when installed too close to the ground. In this case, the low-cost receiver equipped with an AT360 antenna can also provide accurate tropospheric parameters, indicating it as a cost-efficient

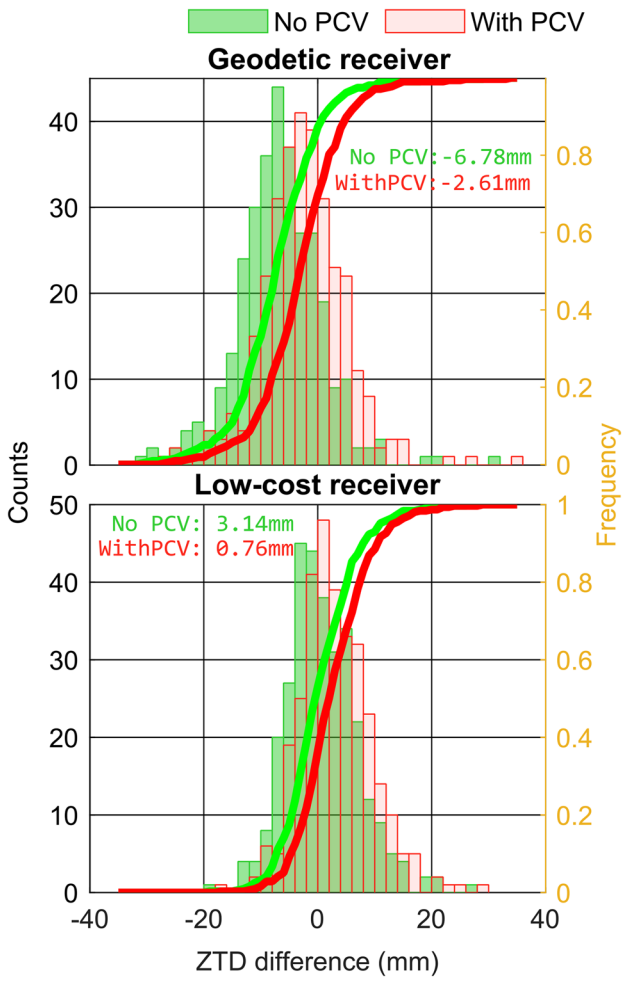

Fig. 2 The cumulative distribution of differenced ZTD (mm) of JFTA (geodetic) and JFSP (low-cost) against CODE, respectively. The antenna on JFTA is TRM159900.00, while the antenna of JFSP is CNTAT360

solution for dense tropospheric monitoring. Additionally, our postprocessing products offer enough accuracy to CODE. We relied on our estimated postprocessing products as evaluation benchmarks in subsequent experiments where CODE tropospheric products are unavailable for reference.

The cross-validation of postprocessing ZTD stems from the stations deployed in Donghu Campus, as shown in Table 3. We note that the differences in STD between all ZTD results are less than 5 mm. The results show that the height differences cause an obvious difference in ZTD when we compare the ZTD between UBUU (geodetic), APMB3S (geodetic), APMB3T (geodetic) and APMM (low-cost). As mentioned in the previous section, the APMB3T and APMM stations are equipped with U35 (lacking PCVs) and AT360 (with known PCVs), respectively. The UBUU and APMB3S stations are equipped with geodetic antennas, the PCVs of which is known. The differences in ZTD RMS and STD of UBUU (geodetic) and the other stations is around 4.5 mm, with the differences being smaller than 3 mm between APMB3T (geodetic receiver + geodetic antenna), APMB3S (geodetic receiver + low-cost antenna), and APMM (geodetic receiver + low-cost antenna). It may result from the height difference of around 15 m between UBUU and the other three stations. Besides, it is not obvious that the lower accuracy is caused by hardware deficiencies from the comparison between APMB3T, APMB3S and APMM, although there are three scenarios, namely, geodetic receivers + low-cost antenna, geodetic receivers + geodetic antennas, and low-cost receivers + low-cost antenna, respectively. It should be noted that the APMB3T is a Septentrio POLARX5TR receiver equipped with an U35 antenna, which lacks PCVs. This station shows slightly higher discrepancies in ZTD than those of other stations when comparing the RMS of differing ZTD. As expected, the result also shows and supports that this cost-efficient approach installed at APMM has a good and comparable performance in retrieving troposphere with geodetic devices.

It can be concluded that geodetic and low-cost receivers equipped with antennas that lack PCVs may suffer from the negative effects of antenna PCVs. Conversely, a low-cost receiver can yield good results using an antenna with known PCVs. We have demonstrated that utilizing a low-cost antenna with known PCVs for a low-cost receiver noticeably enhances the accuracy of tropospheric estimates. This ensures consistency between low-cost ZTD and geodetic ZTD, enabling the densification of the network by introducing low-cost GNSS devices.

Validation of real-time ZTDs estimated by low-cost GNSS receivers and antennas

After discussing the consistency in postprocessing mode for the troposphere between low-cost and geodetic estimates, we aim to investigate the real-time performance of the low-cost receiver during the conducted real-time experiment.

Figure 4 presents real-time ZTD solutions in summer and winter for three nearby stations in Jiufeng Mountain: JFTA (geodetic), JFSP (low-cost), and JFNG (geodetic). A comparison is made with the CODE final troposphere products. The real-time solutions exhibit noisier results compared to the postprocessing products (Fig. 3) due to the relatively coarse RTS orbit and clock corrections.

In the summer campaign, the biases of real-time ZTDs average around 1 mm with respect to CODE, showcasing sufficient accuracy to serve as data input for NWP. The RMS of ZTD differences is less than 11 mm, which provides adequate precision for these applications. Both geodetic and low-cost receivers demonstrate similar performance in real time, with an RMS of around 10 mm compared to CODE

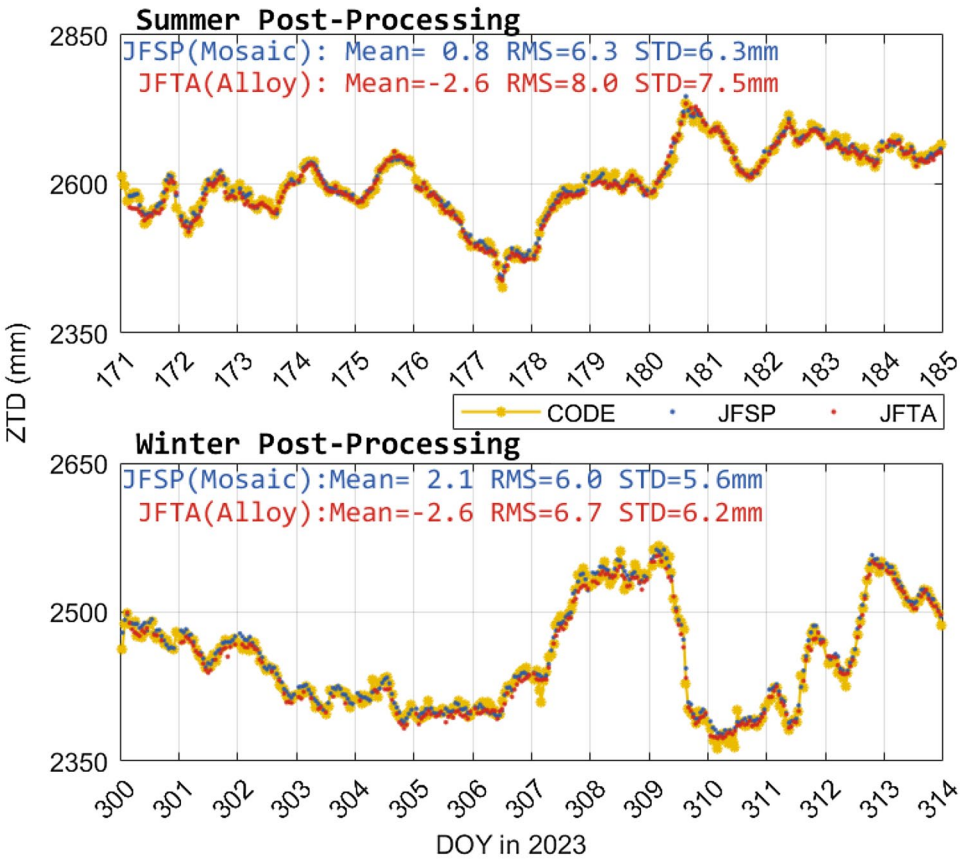

Fig. 3 Time series of the postprocessed GNSS-ZTDs estimated at stations JFSP (low-cost) and JFTA (geodetic) in summer and winter campaign. The CODE final ZTD products for station JFNG are also included as reference. The statistical results for the ZTD differences in terms of mean, RMS, and STD are depicted

Table 3 Cross-comparison results of postprocessing ZTD (mm) from all stations in the Donghu Campus

Stations	APMB3S (GG)	APMB3T (GL)	UBUU (GG)
APMM (LL)	− 1.2, 2.1, 1.7	− 0.4, 3.0, 3.0	2.0, 4.6, 4.2
APMB3S (GG)		0.7, 3.0, 3.0	0.8, 4.4, 4.3
APMB3T (GL)			1.6, 4.4, 4.2

The statistical indicators from left to right are mean (mm), RMS (mm), and STD (mm) of ZTD differences. GG represents the combination of Geodetic receiver and Geodetic antenna, GL represents the combination of Geodetic receiver and Low-cost antenna; LL represents the combination of Low-cost receiver and Low-cost antenna

products. Similarly, in winter, consistency is observed with slightly reduced RMS and STD from both geodetic and low-cost receivers. This could be related to stable variations in the troposphere during winter. Overall, the troposphere in winter is smaller and more stable compared to summer, where occasional heavy rainfall is frequent. This may also be attributed to the random-walk processing noise in the stochastic model of real-time PPP (Wu et al. 2023), due to smaller variations in wet delay in winter.

The impacts of real-time ZTD retrieval between observables and the RTS quality are discussed. RTS plays a more important role in real-time ZTD estimates than the quality of receiver observations. The disruption in DOY 177–179 was mainly attributed to the failure to receive the SSRA00GFZ0 RTS products. Note that the DOY on the horizontal axis represents the end of the day, not the beginning. For example, the time 159.2 in DOY belongs to the day in DOY 160. A disruption in RTS would result in the reconvergence and break the generation of real-time tropospheric estimates.

It can be concluded that low-cost GNSS receivers also have the potential to provide high-quality ZTD results with an RMS of 7–11 mm, showing a similar level of accuracy to geodetic ones. Real-time meteorological applications focus on not only high accuracy but also quick sensing. Therefore, low-cost devices show obvious advantages in this field, serving as a cost-effective means to provide sufficient accuracy of ZTD in (near) real-time.

To further evaluate the quality of the tropospheric estimates from low-cost and geodetic GNSS receivers, the Pearson correlation coefficients (CC) and RMS between the real-time and postprocessing tropospheric estimates from the summer dataset are calculated and the quantile–quantile (QQ) plots are shown in Fig. 5 and Table 4. The real-time solutions show good agreement with the self-postprocessing results at APMB3S, APMB3T, APMM, and UBUU stations,

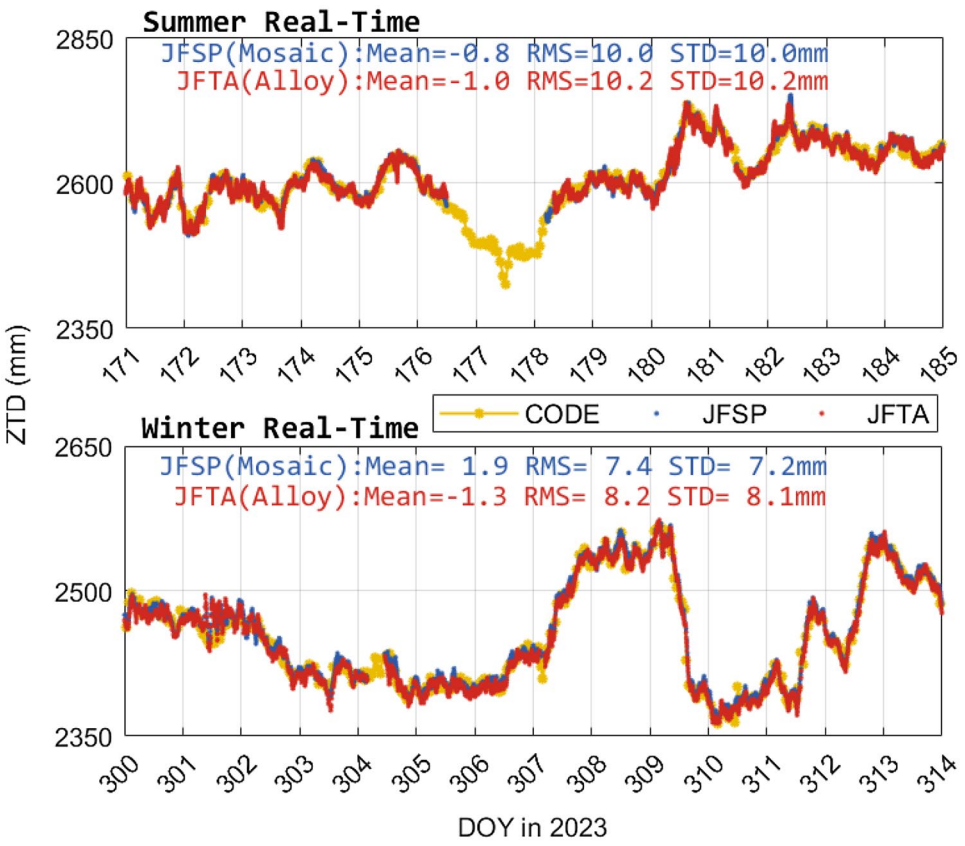

Fig. 4 Time series of the real-time GNSS-ZTDs estimated at stations JFSP (low-cost) and JFTA (geodetic) in summer and winter campaign. The CODE final ZTD products are presented as references. The disruption in DOY 177–179 was mainly attributed to the failure in receiving the SSRA00GFZ0 RTS products

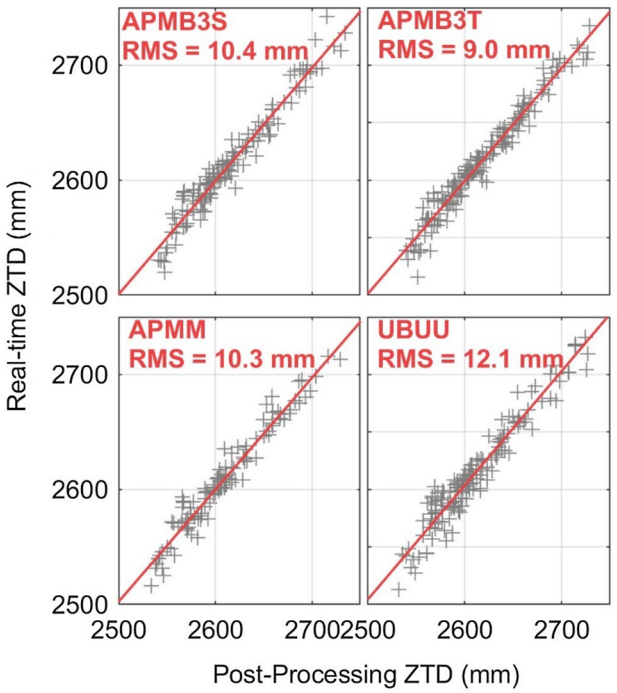

Fig. 5 QQ plots of 4 stations real-time troposphere solutions (mm) with respect to postprocessed troposphere results (mm). The red lines show the linear least squares relationship between the postprocessed solutions and the real-time results

with correlation coefficients above 0.97, and most scatter plots align along the diagonal line (1:1). Even with low-cost GNSS receivers, the agreement in terms of CC falls within the range of 0.96–0.99, demonstrating high consistency between the real-time and postprocessing solutions. However, the low-cost receivers show slightly lower correlations compared to geodetic receivers. As previously mentioned, the APMB3S and APMB3T stations were removed in the winter campaign due to changes in device setup.

Table 4 summarizes the biases, STDs, and RMS of the real-time GNSS-ZTD errors at two low-cost stations (JFSP and APMM) and four geodetic stations in summer and winter campaigns. Overall, the ZTD differences exhibit a slight mean bias with an RMS of around 10 mm. The correlation coefficients, reaching above 0.96, confirm that the real-time results exhibit good agreement with the postprocessing mode in the summer campaign. The STDs of real-time ZTD disparities from the low-cost receivers are similar to those of Trimble and Septentrio receivers, with their RMS ranging from 9 to 12 mm. In winter, the RMS and STD from most stations have reduced to about 8 mm, with around 2 mm in biases. Meanwhile, the CCs between real-time and postprocessed solutions are evident, indicating better performance in sensing ZTD in winter, achieving above 0.99. Low-cost and geodetic devices

Table 4 General statistics of the bias, STD and RMS of the real-time GNSS-ZTDs errors at two low-cost (JFSP and APMM) stations and 4 geodetical stations in summer and winter campaign. The postprocessing ZTDs are used as the references

Station	Mean (mm) Summer/winter	STD (mm) Summer/winter	RMS (mm) Summer/winter	Pearson (CCs) Summer/winter
APMM (low-cost)	0.3/1.3	10.3/6.3	10.3/6.4	0.975/0.993
APMB3S (geodetic)	− 1.0	10.4	10.4	0.986
APMB3T (geodetic)	− 1.0	9.0	9.0	0.981
UBUU (geodetic)	3.6/4.1	12.1/7.3	12.6/8.4	0.992/0.990
JFSP (low-cost)	− 1.4/− 0.3	9.6/7.0	9.6/7.0	0.981/0.991
JFTA (geodetic)	1.8/1.5	12.5/7.9	12.6/8.0	0.961/0.990

demonstrate similar capabilities in capturing ZTD. It can be concluded that the low-cost receivers also achieve high-quality estimates in real-time troposphere sensing.

Real-time ZTD estimations by low-cost GNSS receivers under severe weather conditions

A severe weather event could be detectable by GNSS-ZTDs with a high-updating rate. To show the performance of low-cost GNSS devices in estimating high-updating ZTDs under severe weather conditions, Fig. 6 shows a ZTD response from low-cost GNSS devices during a typical rainfall event. Moreover, ZTDs calculated using geodetic GNSS devices and ERA5 are also presented for comparison. It should be noted that rainfall data refers to the amount of rainfall in the previous entire hour.

The realistic real-time performance of low-cost GNSS devices in typical weather conditions is a main worry and problem in question. The real-time ZTD results from JFSP (low-cost station) are presented in Fig. 6. The results from geodetic receiver (JFTA) are removed for clarity and simplicity. A heavy rain event that exceeds 30 mm/h is recorded by JFSP. The time series from the low-cost station show good consistency with the CODE final product. Notably, there is a visible change in tropospheric ZTD before the rain, followed by a clear drop after the rain. A decrease in ZTD precision and a significant swing in ZTD (refer to the magenta box in Fig. 6) were observed by all receivers before the rain, suggesting a rapid change in humidity. This indicate that the stochastic model in real-time estimation might not suit the changes in tropospheric parameters. It also suggests that tropospheric parameters undergo rapid changes before rainfall, and low-cost receivers can capture these variations. There are slight differences in ZTD recorded by ERA5 during rain events compared to CODE, where the ZTD from ERA5 may be higher than CODE products and exists a bias. It has also been reported that ERA5 exhibits a small moist bias (Stępniak & Paziewski 2022).

Overall, even though the stochastic model might affect the low-cost GNSS tropospheric estimates, they still provide an accurate real-time solution. We believe that the performance in sensing the troposphere during severe weather can be improved with the development of an adaptive model. The low-cost GNSS devices have great potential for use in NWP.

Because there are no nearby IGS and MGEX stations used in CODE products, we also present the real-time results

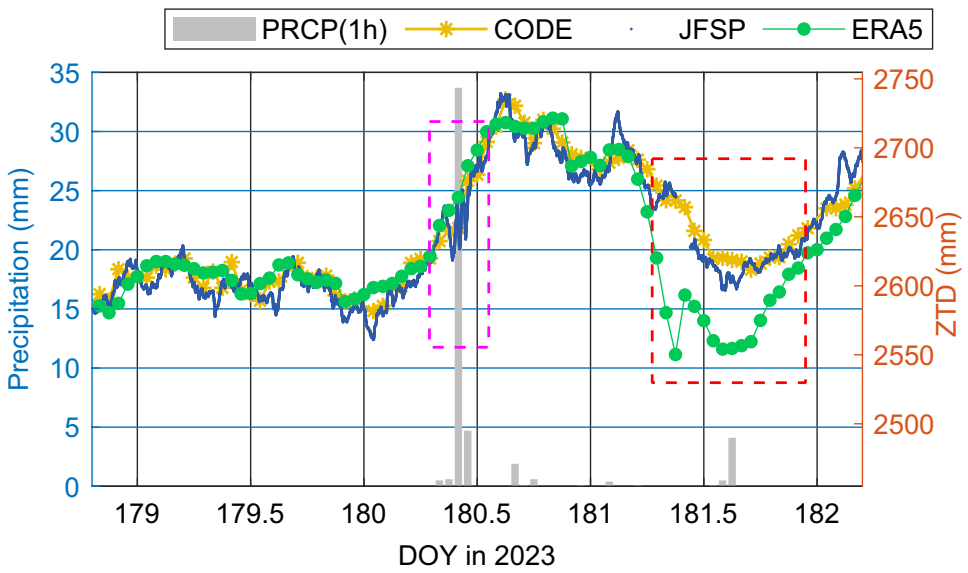

Fig. 6 Real-time ZTD estimates from low-cost receivers JFSP equipped with a mosaic receiver and the result from CODE final products and ERA5 during a rainfall event. The gray column represents hourly precipitation (mm). The left y-axis refers to the one-hourly precipitation depth (mm) from Wuhan meteorological station. The right y-axis refers to the zenith tropospheric delay (mm)

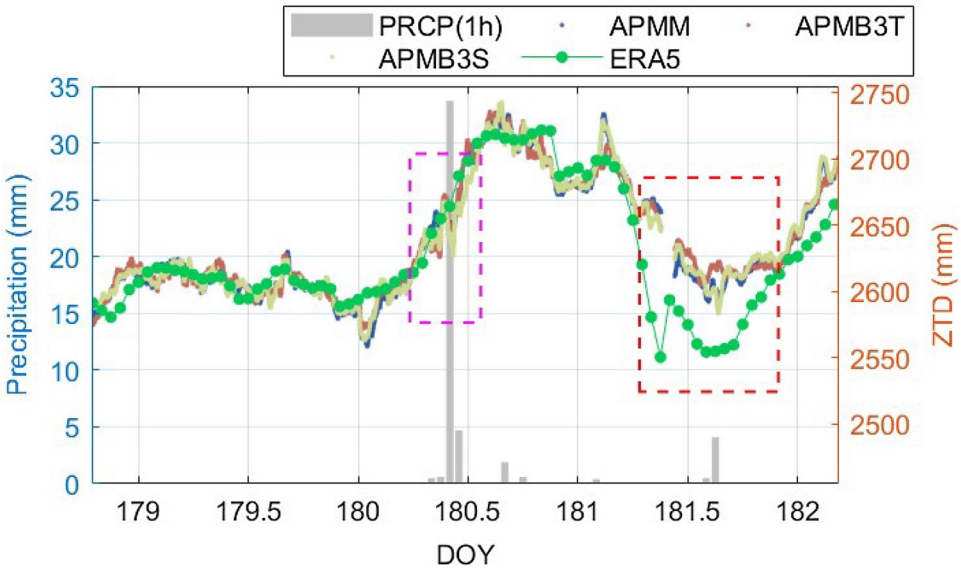

Fig. 7 The real-time ZTD estimates from a low-cost receiver APMM (blue dot) and geodetic receivers APMB3T (brown dot) and APMB3S (cyan dot), which compared with result from ERA5 during a rainfall event. The gray column represents hourly precipitation (mm). The left y-axis refers to the hourly precipitation depth (mm). The right y-axis refers to the zenith tropospheric delay (mm)

of geodetic receivers and ERA5 as reference. As visible in Fig. 7, stations APMB3T (geodetic) and APMM (low-cost) both show the same changes as APMB3S (geodetic), which are deployed in the Donghu Campus. The results from APMB3T equipped with a low-cost antenna lacking PCV have nosier ZTD estimates than the results of APMM (low-cost setup). At the same time, the reinitialization of real-time PPP is observed in DOY 181.3 and the ZTD results of APMM and APMB3T are biased in this stage due the difference in observables. After PPP convergence, the consistency is shown among the three cases. In general, we can notice that high-updating ZTD can be obtained from the real-time streams from low-cost GNSS receivers while the hourly ERA5 products can be accessible with 5 days latency as a typical numerical weather models (NWM) approach. It is a cost-effective way to achieve high-updating water vapor monitoring for a small scale of area using a dense network consisting of low-cost receivers.

Another phenomenon is that ERA5 has an obvious discrepancy of around 40 mm in DOY 182 in contrast to the results from ground-based GNSS in Figs. 6 and 7. This indicates that the tropospheric delays retrieved from ERA5 are occasionally biased over this region. The difference may relate to the interpolation and numerical model when the model is driven by the nature of data assimilated over the lands. However, the real-time ZTD results from low-cost devices are consistent with the CODE final product (see also purple box in Fig. 6). Thus, the real-time tropospheric parameters observed by low-cost GNSS devices can also be used as a valuable data source to verify and rectify the data from NWM.

Low-cost receivers will be a valid alternative for geodetic ones in monitoring networks due to their good performance in real-time regional ZTD sensing. A dense network of low-cost devices can compensate for the low-spatial deficiencies of NWM and better monitoring the troposphere at a small scale. Moreover, jointly using low-cost GNSS stations with current regional GNSS networks is beneficial for GNSS-based tropospheric delay modeling.

Conclusions

We present a study on the real-time tropospheric delay estimations using low-cost GNSS devices. The RTS-based GNSS observations collected by a low-cost GNSS receiver mosaic-X5 ($600) and antenna CNAT360 ($100) is processed in a "true" real-time mode to estimate the real-time zenith tropospheric delays. The performance of the low-cost GNSS device is evaluated by comparing its ZTD results with the references derived from the nearby geodetic GNSS devices in both summer and winter days. The suitability of the low-cost GNSS device for sensing high-updating ZTD variations under severe weather conditions is also analyzed.

First, we find that disregarding PCVs in low-cost GNSS antennas (used in conventional setups with low-cost devices) leads to substantial biases in ZTD estimations. Applying PCVs reduces the ZTD bias by 70%, improving agreement with solutions from geodetic GNSS stations. In postprocessing mode, the low-cost GNSS devices achieve ZTD accuracies of 6.2 mm (in winter) and 7.5 mm (in summer).

Second, in real-time mode, the mean bias of ZTDs in the summer campaign is less than 2 mm with a mean RMS value of 10.8 mm. The results in the winter campaign show a better performance with an average RMS value of 7.5 mm. Even with low-cost GNSS receivers, the solutions highly correlate (0.96–0.99) between real-time and self-postprocessing solutions, indicating near-equivalent performance to

geodetic devices on both accuracy and stability in real-time ZTD estimation.

Third, the results under severe weather events demonstrate that these low-cost GNSS devices capture turbulent ZTD variability, even during rainfall exceeding 30 mm/h. Real-time ZTDs estimated by low-cost GNSS devices can serve as cost-effective data to better support the calibration of NWM and GNSS tropospheric delay modeling.

In conclusion, low-cost GNSS devices (receivers and antennas with PCVs) compete effectively with geodetic ones in estimating real-time ZTDs. These devices and the sensors network consisting of them meet the requirements for real-time atmosphere monitoring and can densify the existing GNSS networks, benefiting atmospheric studies by enhancing the spatial sensing resolution. Future work will focus on utilizing dense low-cost GNSS networks for real-time tropospheric tomography.

Acknowledgements We would like to acknowledge the efforts of GFZ for providing SSRA00GFZ0 products, the Hubei Meteorological Bureau for providing hourly rainfall data and Antenna Calibrations Website of NGS for providing the antenna PCVs. We also thank the European Centre for Medium-Range Weather Forecasts (ECMWF) for online climate data. We also thank the careful check and valuable advice from Dr. Alfred Leick.

Author contributions LL and HZ contributed to conceptualization, methodology, software, and writing—original draft. HZ and YY helped in supervision, project administration, and funding acquisition. MA and BS done supervision, improving the draft, and editing. All authors read and approved the final manuscript.

Funding This work was supported by the National Natural Science Foundation of China (No. 42274043) and the National Key Research & Development Program (No. 2023YFA1009100). The second author was supported by Wuhan Talents Plan (2023). The first author was support by China Scholarship Council (202304910368).

Data availability The reanalysis data provided by the European Centre for Medium-Range Weather Forecasts (ECMWF) are available at https://cds.climate.copernicus.eu. The real-time GNSS-ZTD results can be obtained from the corresponding author.

Declarations

Competing interests The authors declare no competing interests.

Ethical approval Not applicable.

Consent for publication All authors give their consent for publication.

References

Aichinger-Rosenberger M, Wolf A, Senn C, Hohensinn R, Glaner MF, Moeller G, Soja B, Rothacher M (2023) MPG-NET: A low-cost, multi-purpose GNSS co-location station network for environmental monitoring. Measurement 216:112981. https://doi.org/10.1016/j.measurement.2023.112981

Barindelli S, Realini E, Venuti G, Fermi A, Gatti A (2018) Detection of water vapor time variations associated with heavy rain in northern Italy by geodetic and low-cost GNSS receivers. Earth, Planets Space 70:1–8. https://doi.org/10.1186/s40623-018-0795-7

Bevis M, Businger S, Herring TA, Rocken C, Anthes RA, Ware RH (1992) GPS meteorology: remote sensing of atmospheric water vapor using the global positioning system. J Geophys Res Atmos 97:15787–15801. https://doi.org/10.1029/92JD01517

Bosser P, Bennini V, Bouasria M, Grit Y, Panetier A (2022) A low-cost GNSS buoy for water vapour monitoring over the Oceans. In: EGU general assembly conference abstracts. 10.5194/egusphere-egu22-1811

Bosser P, Ancelin J, Métois M, Rolland L, Vidal M. (2023). Water vapour monitoring over France using the low-cost GNSS collaborative network Centipede. In: EGU general assembly.

Chen G, Herring T (1997) Effects of atmospheric azimuthal asymmetry on the analysis of space geodetic data. J Geophys Res Solid Earth 102:20489–20502

Dach R, Brockmann E, Schaer S, Beutler G, Meindl M, Prange L, Bock H, Jäggi A, Ostini L (2009) GNSS processing at CODE: status report. J Geodesy 83:353–365. https://doi.org/10.1007/s00190-008-0281-2

Dousa J, Vaclavovic P (2014) Real-time zenith tropospheric delays in support of numerical weather prediction applications. Adv Space Res 53:1347–1358. https://doi.org/10.1016/j.asr.2014.02.021

Du Z, Zhao Q, Yao Y, Zhu H (2023) Real-time tropospheric delay map retrieval using sparse GNSS stations. GPS Solut 28(1):12. https://doi.org/10.1007/s10291-023-01554-x

Gendt G, Dick G, Reigber C, Tomassini M, Liu YX, Ramatschi M (2004) Near real time GPS water vapor monitoring for numerical weather prediction in Germany. J Meteorol Soc Jpn 82:361–370. https://doi.org/10.2151/jmsj.2004.361

Guerova G et al (2016) Review of the state of the art and future prospects of the ground-based GNSS meteorology in Europe. Atmos Meas Tech 9:5385–5406. https://doi.org/10.5194/amt-9-5385-2016

Hadas T, Hobiger T, Hordyniec P (2020) Considering different recent advancements in GNSS on real-time zenith troposphere estimates. GPS Solut 24(4):99. https://doi.org/10.1007/s10291-020-01014-w

Hersbach H et al (2020) The ERA5 global reanalysis. Q J R Meteorol Soc 146:1999–2049. https://doi.org/10.1002/qj.3803

Huang L, Mo Z, Xie S, Liu L, Chen J, Kang C, Wang S (2021) Spatiotemporal characteristics of GNSS-derived precipitable water vapor during heavy rainfall events in Guilin, China. Satell Navig 2:1–17

Humphrey V, Frankenberg C (2023) Continuous ground monitoring of vegetation optical depth and water content with GPS signals. Biogeosciences 20:1789–1811. https://doi.org/10.5194/bg-20-1789-2023

Jones J, Guerova G, Douša J, Dick G, de Haan S, Pottiaux E, Bock O, Pacione R, Van Malderen R (2020) Advanced GNSS tropospheric products for monitoring severe weather events and climate. https://doi.org/10.1007/978-3-030-13901-8.pdf

Karegar MA, Kusche J, Geremia-Nievinski F, Larson KM (2022) Raspberry Pi reflector (RPR): a low-cost water-level monitoring system based on GNSS interferometric reflectometry. Water Resour Res. https://doi.org/10.1029/2021wr031713

Krietemeyer A, M-c TV, Van der Marel H, Realini E, Van de Giesen N (2018) Potential of cost-efficient single frequency GNSS receivers for water vapor monitoring. Remote Sens 10(9):1493. https://doi.org/10.3390/rs10091493

Krietemeyer A, van der Marel H, van de Giesen N, Ten Veldhuis MC (2020) High quality zenith tropospheric delay estimation using a low-cost dual-frequency receiver and relative antenna calibration. Remote Sens 12(9):1393. https://doi.org/10.3390/rs12091393

Li X, Zus F, Lu C, Dick G, Ning T, Ge M, Wickert J, Schuh H (2015) Retrieving of atmospheric parameters from multi-GNSS in real time: validation with water vapor radiometer and numerical weather model. J Geophys Res: Atmos 120:7189–7204. https://doi.org/10.1002/2015jd023454

Lu C, Zus F, Ge M, Heinkelmann R, Dick G, Wickert J, Schuh H (2016) Tropospheric delay parameters from numerical weather models for multi-GNSS precise positioning. Atmos Meas Tech 9:5965–5973. https://doi.org/10.5194/amt-9-5965-2016

Lu C, Zhong Y, Wu Z, Zheng Y, Wang Q (2023) A tropospheric delay model to integrate ERA5 and GNSS reference network for mountainous areas: application to precise point positioning. GPS Solut 27(2):81. https://doi.org/10.1007/s10291-023-01425-5

Marut G, Hadas T, Kaplon J, Trzcina E, Rohm W (2022) Monitoring the water vapor content at high spatio-temporal resolution using a network of low-cost multi-GNSS Receivers. IEEE Trans Geosci Remote Sens 60:1–14. https://doi.org/10.1109/tgrs.2022.3226631

Moeller G (2022) Nanosatellites: The next big chapter in atmospheric tomography. In: Inverse problems-recent advances and applications [Working Title]. IntechOpen.

Paziewski J (2021) Multi-constellation single-frequency ionospheric-free precise point positioning with low-cost receivers. GPS Solut 26(1):23. https://doi.org/10.1007/s10291-021-01209-9

Perspectives of Cost-Efficient GNSS Equipment for Wide-Spread and High-Quality Meteorological and Positioning Applications.

Pottiaux E. (2009). GNSS near real-time zenith path delay estimations at rob: Methodology and quality monitoring. Bulletin of Geodesy and Geomatics, 125–146.

Stępniak K, Paziewski J (2022) On the quality of tropospheric estimates from low-cost GNSS receiver data processing. Measurement 198:111350. https://doi.org/10.1016/j.measurement.2022.111350

Wang J, Balidakis K, Zus F, Chang X, Ge M, Heinkelmann R, Schuh H (2022) Improving the vertical modeling of tropospheric delay. Geophys Res Lett 49(5):e2021GL096732. https://doi.org/10.1029/2021gl096732

Wilgan K, Dick G, Zus F, Wickert J (2023) Tropospheric parameters from multi-GNSS and numerical weather models: case study of severe precipitation and flooding in Germany in July 2021. GPS Solut 27(1):49. https://doi.org/10.1007/s10291-022-01379-0

Wu Z, Lu C, Lyu H, Han X, Zheng Y, Liu Y, Liu Y, Jin K (2022) Sensing real-time water vapor over oceans with low-cost GNSS receivers. IEEE Trans Geosci Remote Sens 60:1–8. https://doi.org/10.1109/tgrs.2022.3213427

Wu Z, Lu C, Tan Y, Zheng Y, Liu Y, Liu Y, Jin K (2023) Real-time GNSS tropospheric delay estimation with a novel global random walk processing noise model (GRM). J Geod 97(12):112. https://doi.org/10.1007/s00190-023-01780-8

Zangenehnejad F, Gao Y (2021) GNSS smartphones positioning: advances, challenges, opportunities, and future perspectives. Satell Navig 2:24. https://doi.org/10.1186/s43020-021-00054-y

Zhang H, Yuan Y, Li W (2022) Real-time wide-area precise tropospheric corrections (WAPTCs) jointly using GNSS and NWP forecasts for China. J Geod 96(6):44. https://doi.org/10.1007/s00190-022-01630-z

Zhao C, Zhang B, Zhang X (2021) SUPREME: an open-source single-frequency uncombined precise point positioning software. GPS Solut 25(3):86. https://doi.org/10.1007/s10291-021-01131-0

Luohong Li is currently pursuing a Ph.D. degree at the Innovation Academy for Precision Measurement Science and Technology (APM), Chinese Academy of Sciences (CAS), Wuhan, China. His research focuses on GNSS atmosphere monitoring with low-cost GNSS sensors.

Hongxing Zhang is currently an associate professor at APM, CAS. He received his Ph.D. from the Institute of Geodesy and Geophysics, Chinese Academy of Sciences in 2019. His research focuses on neutral atmosphere effects in space geodesy and GNSS-based precise tropospheric modeling.

Yunbin Yuan is a professor and the director of the GNSS Research Group at APM, CAS. His current research interests include GNSS-based spatial

environmental monitoring and high-precision GNSS navigation and positioning

Matthias Aichinger-Rosenberger is currently a post-doctoral scientist in space geodesy at ETH Zurich. He received his PhD degree from TU Wien in 2021. His main research interests are GNSS and their manifold applications for remote sensing (GNSS-RS), meteorology (data assimilation), and environmental monitoring.

Benedikt Soja is currently an assistant professor of space geodesy at ETH Zurich. He received his Ph.D. degree from TU Wien in 2016. His current research focuses on GNSS data processing and machine learning applications in geodesy.